Formation of helium-bubble networks in tungsten

Luis Sandoval[a,1], Danny Perez[a], Blas P. Uberuaga[b], Arthur F. Voter[a]

[a] *Theoretical Division, Los Alamos National Laboratory, Los Alamos, NM 87545, USA*
[b] *Materials Science and Technology Division, Los Alamos National Laboratory, Los Alamos, NM 87545 USA*

Abstract

The nucleation and subsequent growth of helium bubbles in bulk tungsten is investigated using molecular dynamics simulations. By considering a setting that includes the diffusion process of helium clusters, we study their attachment to existing bubbles and their interaction with tungsten crowdion structures generated in the bubble growth process. We find that incoming helium atoms, and especially small helium clusters, can become trapped in the crowdion structures, providing nucleation sites for new helium bubbles, and leading to a distributed network of bubbles rather than a single, growing bubble. The nature of this network depends on both the temperature and the implantation flux of helium. Our results indicate that the kinetic interaction of He with generated dislocations is a key factor dictating the evolution of bubble distributions in plasma-exposed tungsten.

Keywords: Tungsten, Nucleation and growth, Molecular dynamics

1. Introduction

Tungsten is a leading candidate as a surface material for magnetic confinement fusion reactors [1, 2], mainly due to its favorable plasma-facing properties: low hydrogen solubility, low sputtering yield, high melting point, and high thermal conductivity [3]. Despite these attractive attributes, the material is still significantly affected by the plasma and fusion by-products. One key issue is the formation of a "fuzz"-like nanostructure that develops on the surface [4], whose origin has been ascribed to the nucleation and growth of helium bubbles [5], but whose precise formation mechanism, in particular the dependence on temperature, remains the subject of much debate.

Under the conditions expected in the ITER's divertor, low-energy helium ions ($\lesssim 100\,\mathrm{eV}$) impact a high-temperature tungsten surface ($\sim 1000\,\mathrm{K}$) [6].

Email addresses: danny_perez@lanl.gov (Danny Perez), blas@lanl.gov (Blas P. Uberuaga)

[1] Present address: AMA Inc., Thermal Protection Materials Branch, NASA Ames Research Center, Moffett Field, California, 94035, USA.

Approximately two thirds of these particles are desorbed from the surface after contact; the rest penetrate the material defining a depth distribution with a mean value of $\sim 1\,\mathrm{nm}$ [7]. The maximum energy transferable from the collision is significantly below the tungsten displacement threshold [8], so no tungsten defects are created during the actual impact. After a non-thermal transient phase ($\sim 1\,\mathrm{ps}$ [7]), the helium atoms start to diffuse. Eventually they form helium clusters, which diffuse at lower rates, depending on cluster size [9]. At a critical helium content ($\sim 8\,\mathrm{He}$ atoms) a trap mutation event triggers the nucleation of a Frenkel pair [10]. The entity composed by the helium cluster, the tungsten interstitial (crowdion) and vacancy, practically immobile under molecular dynamics (MD) time scales, is the seed that produces a helium bubble by additional attachment of diffusing helium clusters. As the content of helium atoms in the bubble increases, more Frenkel pairs are nucleated: new tungsten vacancies allow the helium bubble to grow, and the tungsten interstitials form a $\langle 111 \rangle$ dislocation line attached to the bubble; that is, the ends of the dislocation line are touching the bubble. After some time the dislocation detaches from the bubble as a (closed) loop, which, if close to the surface, can displace tungsten atoms toward the surface [11, 12, 13].

Recently it was highlighted that the interaction of helium clusters with relatively large helium bubbles is far from a trivial process [14]. It was shown that trap mutation is enhanced in the bubble's neighborhood, which facilitates the nucleation of "satellite" bubbles from He clusters that would be sub-critical in bulk. These bubbles are subsequently absorbed or annihilated by the larger pre-existing bubble. While the bubbles were "clean" in the aforementioned study, i.e., free of bound tungsten interstitials, the role of defects has also been considered. Experimentally, it was suggested that all of the entrapment of He occurs at vacancies [15]; however, recent simulations have revealed a more complex scenario. Juslin et al. [16] observed the binding of helium to tungsten interstitials, reducing the mobility of both defects. Kobayashi et al. [17] highlighted a self-induced bubble growth mechanism where small bubbles become arranged along the $\langle 111 \rangle$ direction in a short period of time. Smirnov et al. [18] showed that the dislocations loops bound to a bubble also can trap helium atoms as they slip and serve as precipitation locations for formation of new bubbles. Krasheninnikov and Smirnov [19] presented a theoretical model describing the helium cluster evolution in tungsten taking into account the role of helium traps generated in the bubble growth process, specifically dislocation lines. Motivated by these results, we here investigate the interaction between growing bubbles, potentially decorated by tungsten interstitials, and incoming helium clusters. We find that the interaction of incoming He with the dislocation lines emitted by overpressurized bubbles leads to He trapping, which can enhance the nucleation of new bubbles in their vicinity. Critically, this effect depends on the temperature, indicating that the bubble network that forms is very sensitive to the conditions within the material.

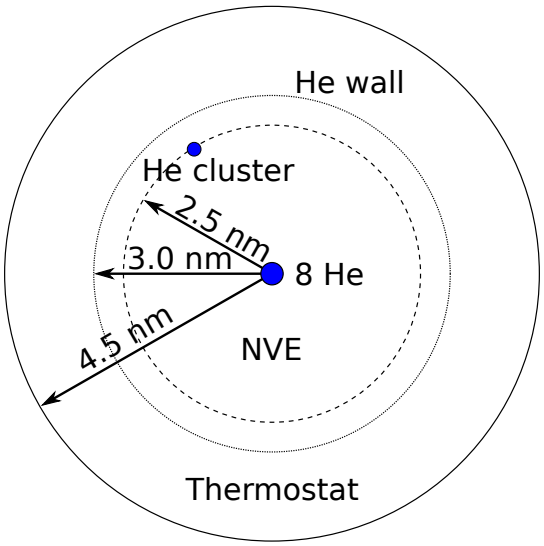

Figure 1: Simulation setup: A cluster containing eight helium atoms is located at the center of a tungsten sphere with a radius of 4.5 nm (23538 tungsten atoms). The helium cluster is large enough to easily nucleate a tungsten Frenkel pair via the self-trapping mechanism. At 3 nm from the center a spherical reflective wall is defined affecting only helium atoms. The wall also separates the exterior thermostated region from the central region where the atoms evolve according to the micro-canonical ensemble. New helium atoms are introduced in the system at a distance of 2.5 nm from the center, randomly on the corresponding spherical shell.

2. Methodology

The simulation setup is described in Fig. 1. A cluster containing eight helium atoms is located at the center of a tungsten sphere with a radius of 4.5 nm (23538 tungsten atoms). This helium cluster is large enough to easily nucleate a tungsten Frenkel pair via self-trapping, which happens during the first picoseconds of the 1-ns equilibration period. A spherical reflective wall that affects only helium atoms, (whose purpose is to maintain a prescribed density of He atoms by preventing their escape from the simulation region) is imposed 3 nm away from the center. The wall also separates the exterior thermostated (via Langevin dynamics) zone from the central region where the atoms evolve according to the micro-canonical ensemble. New helium atoms are introduced in the system at a distance of 2.5 nm from the center, randomly positioned on the corresponding spherical shell. Note that this setup is designed to simulate bulk-like conditions, that is, evolution of deep helium bubbles. We have considered the insertion of only monomers (single helium atoms) and dimers, having in mind a situation close to experimental conditions where monomers dominate the population of clusters diffusing in the tungsten matrix [20]. The insertion rate has been fixed to 1×10^9 He s^{-1}, which we found to be slow enough to allow one cluster at a time to diffuse and interact with the central bubble. We have focused on the temperature range from 600 K to 2000 K, which includes the temperatures expected at ITER [21]. Molecular dynamics (MD) simulations were performed with the open source code LAMMPS [22]. The interaction between W atoms is determined by an Ackland-Thetford potential [23], modified at short distances by Juslin and Wirth [24]. He-W interactions were obtained from Juslin and Wirth [24], while the He-He potential corresponds to the one used by Beck [25] modified at short distances by Morishita et al. [26]. Tungsten point defects are detected by the Wigner-Seitz analysis as implemented in OVITO [27].

3. Results and Discussion

To highlight the main features observed in the simulations, we first discuss simulations at 1000 K where only monomers were inserted. Representative snapshots are shown in Fig. 2. In this work we consider the term *helium cluster* as a synonym of *mobile* helium *interstitial* cluster, and *helium bubble* as a conglomerate of helium atoms located in one or more tungsten vacancies, an entity practically immobile at the time-scales considered here, but which were recently shown to be able to move on longer timescales [28].

First, a helium bubble and a tungsten interstitial are formed via self-trapping from the initial helium cluster located at the center, approximately 25 ps after the simulation starts. The corresponding tungsten crowdion changes directions as the tungsten interstitial diffuses around the helium bubble with a hopping frequency of $\sim 10^{10}$ s^{-1} [29]. New He atoms, inserted at a rate of 1×10^9 He s^{-1}, attach to the bubble, increasing the bubble pressure until a second Frenkel pair

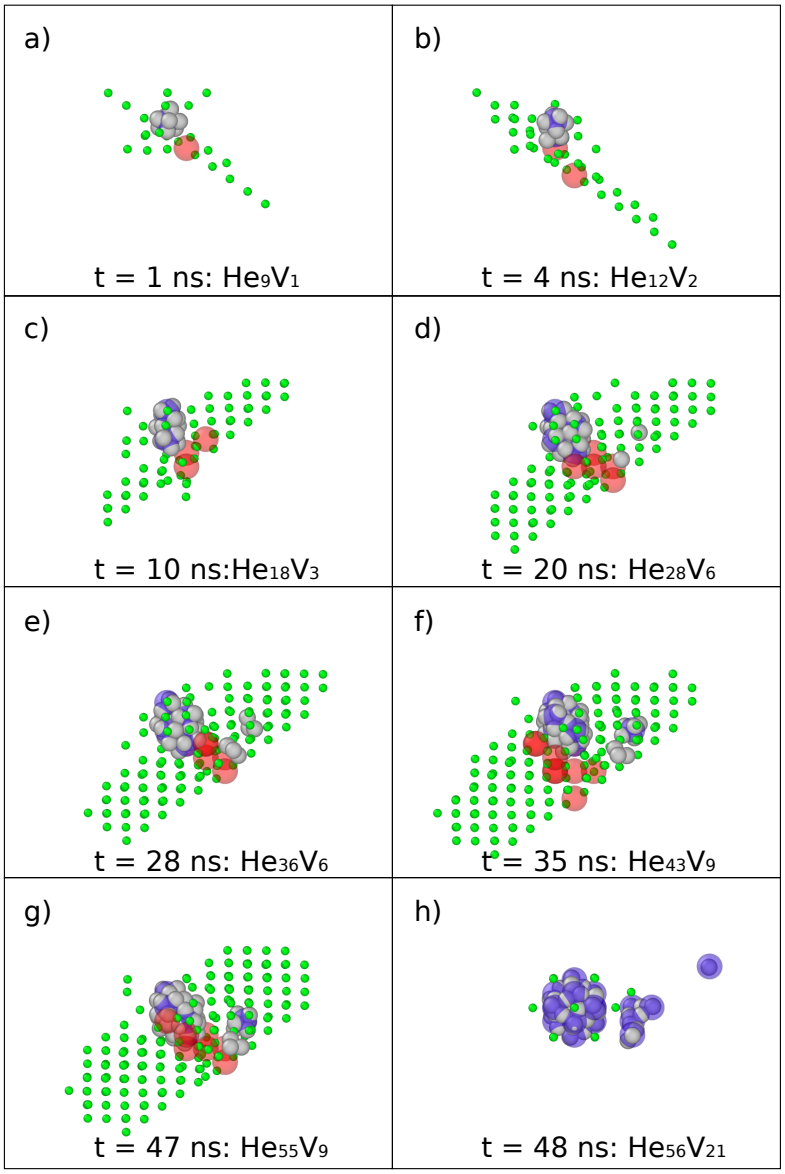

Figure 2: Formation of a bubble network at T = 1000 K corresponding to an insertion rate of 1×10^9 He s^{-1}. Here, helium atoms are gray, tungsten interstitials are red, and tungsten vacancies blue. We have also highlighted with green the tungsten atoms corresponding to the deformed lattice around tungsten interstitials (crowdions).

is nucleated, as shown in Fig. 2(a-b). The two crowdions now diffuse in a coordinated way around the bubble, keeping the same orientation in adjacent $\langle 111 \rangle$ rows. Note that these two tungsten interstitials form an incipient dislocation line attached to the bubble. After new helium atoms are captured by the bubble a third Frenkel pair is nucleated. At this stage, the crowdions become less mobile, rarely changing orientation over simulation timescales (Fig. 2(c)). Incoming helium atoms are observed to interact with the bubble (being captured), or with the crowdion structure (being temporarily trapped) as shown in Fig. 2(d). Helium atoms trapped in the crowdion structure are not completely immobilized, as they can diffuse along the crowdions or even jump to the helium bubble; however, for the temperature and insertion rate studied here, these helium atoms can also act as nucleation centers for new bubbles, as shown in Fig. 2(e-g). That is, whether they first reach the existing bubble or form the nucleus of a new bubble depends on their mobility relative to the arrival rate of additional He to the region. Subsequently inserted helium atoms now can be either captured by the original bubble, captured by the clusters or bubbles nucleated in the crowdion structure, or trapped by the crowdions themselves. Eventually, the crowdion structure can detach from the bubble conglomerate, leaving behind a clean bubble network, as shown in Fig. 2(h). In this final structure, there are three distinct bubbles separated spatially from one another. Thus, the interaction of incoming helium with the tungsten interstitial structure around the first bubble leads to a more complex network of small helium bubbles rather than a single growing bubble.

To understand the importance of the relative He rates (arrival versus migration and trapping/detrapping in the bubble region) that drive the kinetic evolution of this system, we also performed simulations at different temperatures (600 K, 700 K, ..., 2000 K), considering two insertion modes: only monomers, and a mixed insertion of monomers and dimers [20] (where dimers were inserted 20 times less often than monomers). For each of the 15 temperatures and two insertion modes, we performed two simulations with different random seeds for the Langevin thermostat, for a total of 60 simulations. In Fig. 3 we show representative snapshots corresponding to the final state (after 55 helium atoms were inserted). These snapshots show a marked difference in the number of bubbles and clusters trapped by the evolving crowdion structure as a function of temperature. As the temperature is increased, helium atoms are more likely to find existing bubbles than becoming trapped by the crowdions for long enough that a new bubble is nucleated. At the highest temperature, only one bubble is formed. This behaviour is in close agreement with experimental results where smaller helium bubbles are observed at lower temperatures [30, 31]. To quantify this apparent trend, Fig. 4 reports the number of helium clusters and bubbles as a function of the temperature, after 55 helium atoms have been inserted. Two helium-insertion modes have been considered (two simulations per insertion mode): only monomers at a rate of 1×10^9 He s^{-1} (blue circles), and monomers (same rate) plus three dimers inserted at $\mathrm{t} = 10, 30, \text{and } 50$ ns. The results show a clear temperature effect on the process of bubble formation via trapping of helium clusters in the crowdion structures induced by growing

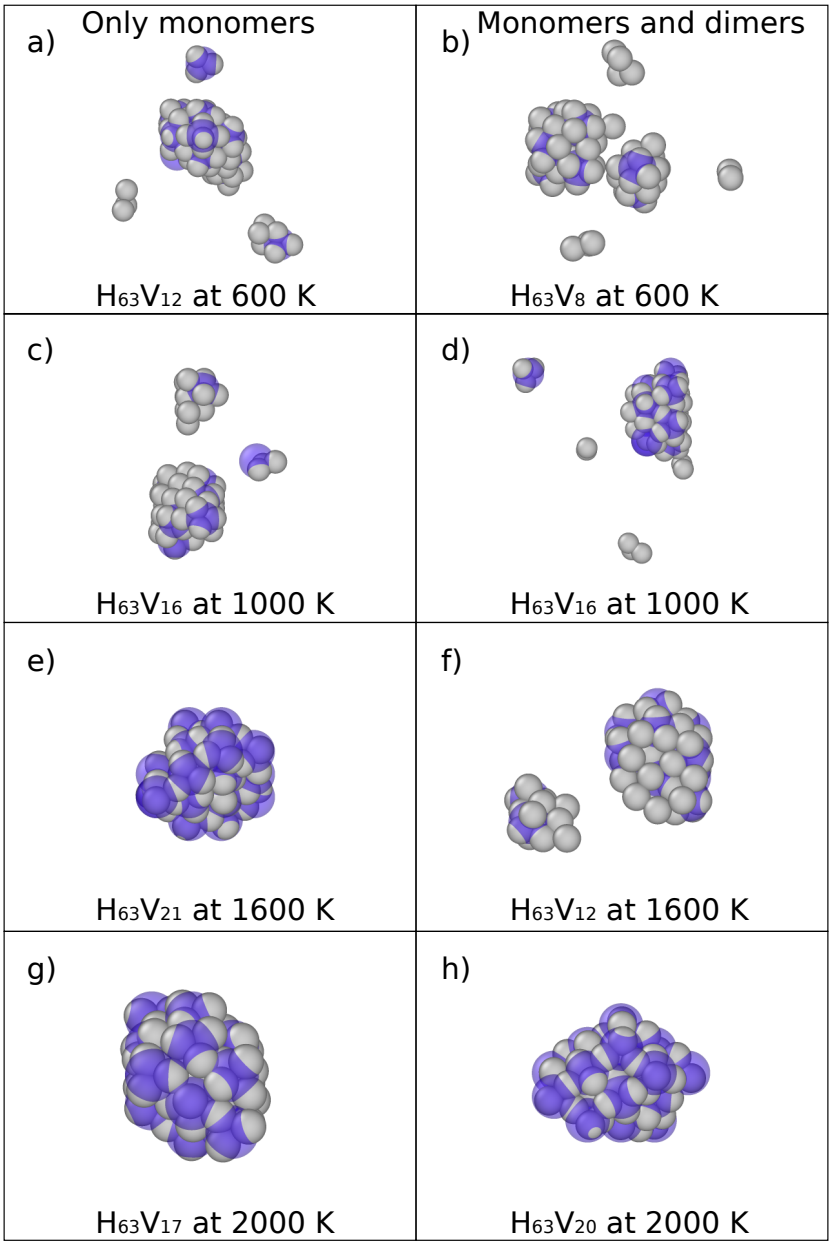

Figure 3: Formation of bubble networks at different temperatures and helium-insertion conditions. The left column shows snapshots after insertion of 55 helium monomers at a rate of 1×10^9 He s^{-1}. For comparison, the right column shows snapshots after 49 helium monomers have been inserted, also at 1×10^9 He s^{-1}, plus three helium dimers inserted at t = 10, 30, and 50 ns (we allow 2 ns for dimer diffusion before inserting the next monomer). As before, helium atoms and tungsten vacancies are denoted by gray and blue spheres, respectively.

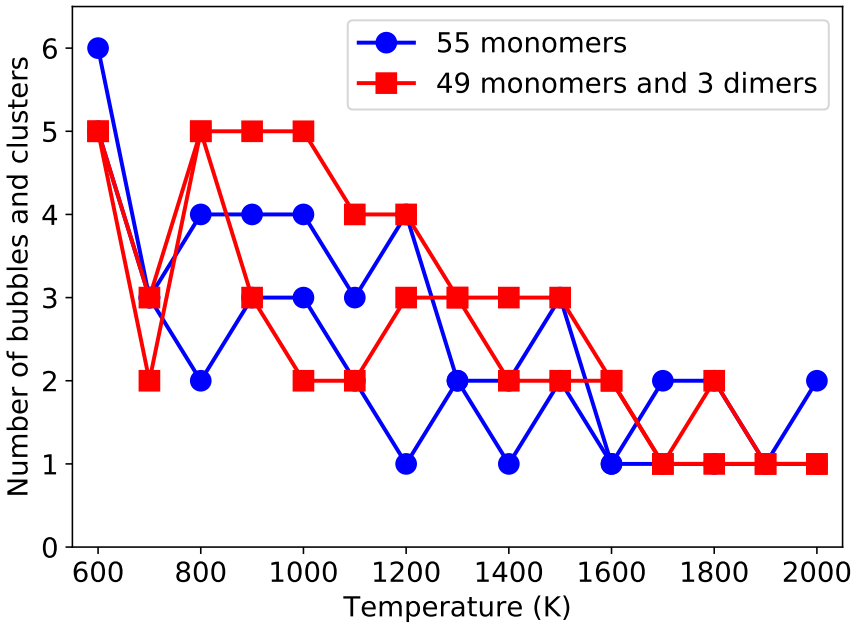

Figure 4: Number of helium clusters and bubbles, as a function of the temperature, once 55 helium atoms have been inserted. Two helium-insertion modes have been considered (two simulations per insertion mode): only monomers at a rate of 1×10^9 He s^{-1} (blue circles), and monomers (same rate) plus three dimers inserted at t = 10, 30, and 50 ns (red squares).

bubbles. Also, the simulations with dimers included indicate a slight increase in the numbers of nucleated clusters and bubbles, suggesting that the nature of the incoming He further modifies the balance of rates that dictate the formation of the bubble network. However, more simulations are required to precisely quantify this effect.

The previous simulations clearly show that, once a crowdion structure develops around a bubble, it interacts with incoming helium, either impeding its ability to find the central bubble or even trapping it. To examine this behavior in more detail, we have simulated the interaction between isolated crowdions and helium interstitial clusters. We have considered eight cases corresponding to one or two crowdions interacting with clusters containing one to four helium atoms. For these simulations, the tungsten interstitials and the helium atoms are inserted in a bcc tungsten periodic lattice containing 8640 atoms. Their initial separation is 1 nm. After 10 ps of equilibration at 1000 K and 0 GPa, the system evolves according to the microcanonical ensemble for 10 ns. We find that the interaction between a helium atom and a single tungsten crowdion is relatively weak, as the average trapping time (the time until the two entities come apart) is $\sim$ 100 ps. The average trapping time for a helium atom and

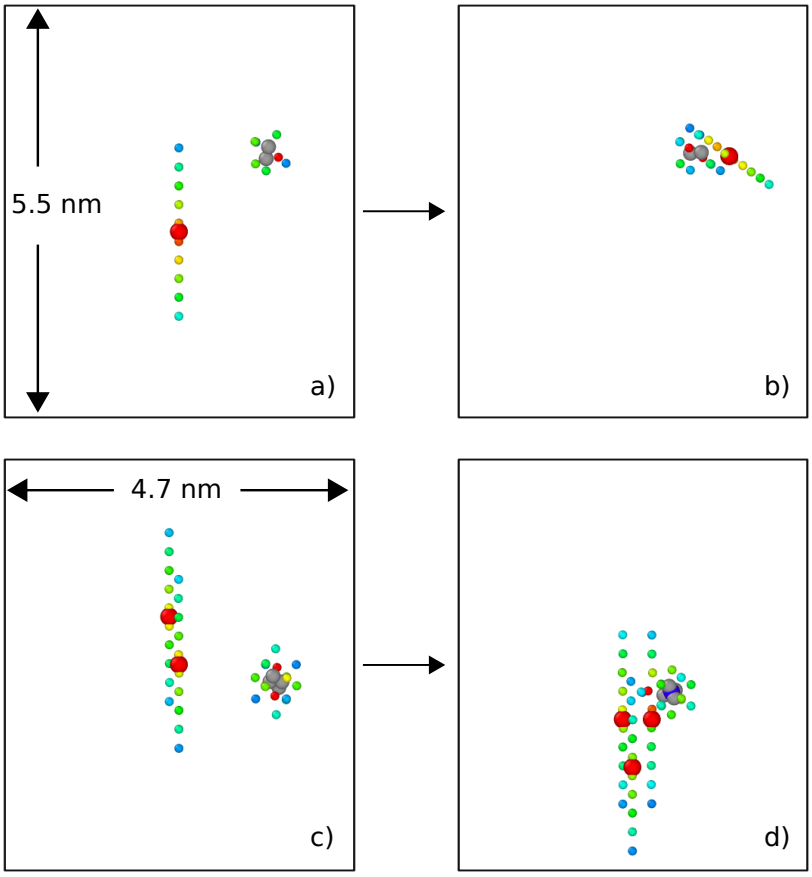

Figure 5: Interaction between tungsten crowdions and helium clusters at 1000 K. The top snapshots show a single tungsten crowdion and a helium dimer, both diffusing in a perfect tungsten lattice. The bottom left snapshot shows two adjacent crowdions, and a helium cluster containing four helium atoms, whose interaction is able to nucleate a Frenkel pair (an additional crowdion and a vacancy). Helium atoms, tungsten interstitials, and tungsten vacancies are denoted by gray, red and blue spheres, respectively. We have also highlighted the tungsten atoms corresponding to the deformed lattice around tungsten interstitials (crowdions).

Crowdions	1 He	2 He	3 He	4 He
1 (this work)	0.44	0.60	0.83	1.15
1 (DFT [32])	1.03	1.06	1.63	2.24
2 (this work)	0.44	1.01	1.59	1.96

Table 1: Binding energies, in eV, of helium clusters to a single crowdion (first row), and two contiguous crowdions (third row), as determined by the classical potentials used in this work. In order to calculate these values, we subtract the energy of a (minimized) system containing the helium cluster attached to the crowdion(s), from the energy of a system where crowdion(s) and helium cluster are separated (the simulation box, containing $\sim$ 16000 atoms, was big enough to avoid interaction). On the second row we show DFT data from Ref. [32].

two adjacent crowdions is similar, at around 200 ps. In contrast, there is a quite strong interaction between helium clusters containing two, three or four atoms, and single or double crowdions; in this case the average trapping time is larger than the simulated time of 10 ns. Representative snapshots are shown in Fig. 5(a-d). We can rationalize this behaviour by considering the binding energies of helium clusters to the crowdions, which are presented in Table 1. A crude approximation *via* an Arrhenius expression with a pre-factor of 1×10^{12} s provides values within an order of magnitude of the finite-temperature simulations, in particular for the interaction of a single helium atom and the crowdions (165 ps for a binding energy of 0.44 eV). In Table 1 we also present DFT results from Ref. [32] for the case with a single tungsten crowdion. Note that the binding energies from the classical potentials are approximately half of those reported in Ref. [32], indicating that our simulations would underestimate the effects observed (time-scales, the role of temperature, topology of the bubble networks, etc.). However, the overall physical behavior as described by DFT-quality interactions would be similar to that predicted here. Interestingly, the interaction between two adjacent crowdions and a 4-atom helium cluster is strong enough to nucleate a Frenkel pair, generating an additional crowdion and a tungsten vacancy where the helium atoms get trapped (see Fig. 5(d)); that is, the presence of crowdions can induce self-trapping at smaller helium cluster sizes than possible in perfect bulk tungsten.

Taking all of our simulations together, we are led to the following picture of bubble nucleation in tungsten: If a single helium atom temporarily trapped in the crowdion structure (two or more tungsten interstitials) remains trapped long enough, without being captured by the existing bubble, it can eventually be joined by a newly inserted helium atom, forming a dimer whose interaction with the crowdion structure is even stronger. Once the dimer captures two additional helium atoms, a Frenkel pair might be formed (as seen in Fig. 5(d)), nucleating a new helium bubble by self-trapping. The process continues as new bubbles capture helium atoms, generating more crowdions around them, which, in turn, can capture diffusing helium atoms. The long term result is the formation of a network of smaller, more dispersed helium bubbles. These results also suggest that if the relative population of He dimers increases, the number of trapped clusters in the bubble network also increases, as they are more easily trapped by

the crowdion structure. This would explain the observed trend of fewer trapped clusters and nucleated bubbles in the monomer-only insertion simulations as compared to the insertion mode where three dimers have been included. Finally, if the trapping time of helium by crowdions is decreased, e.g. by raising the temperature, the probability of helium interstitials reaching the existing bubbles increases, leading to the formation of fewer but larger bubbles. Thus, the nature of the bubble network that is formed is sensitive to the various competing rates in the system, and the dominant rate is a function of temperature.

We highlight here two possible factors affecting the evolution of the bubble network. First, as bubbles in the network get large, they could potentially capture the neighboring "satellite" bubbles, as shown in Ref. [14]. This depends on the ability of helium to reach these bubbles and not be trapped before it gets there. Also, note that the formation of the bubble network would depend on the helium flux. If the helium flux is low, the density of helium atoms diffusing in the tungsten matrix decreases, which means that the helium clusters trapped in crowdion structures would presumably have time to de-trap, making the formation of the network dificult. Thus not only temperature but the implantation flux will dictate the nature of the final bubble network.

Finally, it is intriguing to note that the temperature dependence of the network formation is similar to that of fuzz formation, hinting at a potential link, though more work is needed to establish a definitive connection.

4. Conclusions

Using molecular dynamics simulations we have investigated the early stages of helium bubble growth in tungsten following the self-trapping that first brings the bubble into existence. Crowdion structures generated around the initial bubble are able to trap incoming diffusing helium clusters. Helium monomers can interact with single or double crowdions for hundreds of picoseconds without being captured by the bubble. Even stronger interactions with the crowdions are observed if the helium clusters contain two or more atoms; these clusters are trapped for many nanoseconds, acting as new attachment centers for diffusing helium atoms. According to our simulations, a trapped cluster containing just four helium atoms can nucleate a Frenkel pair, increasing by one the number of crowdions, and creating a new bubble. This crowdion-assisted bubble nucleation process continues, creating a bubble network. We have also observed a clear temperature dependence; the propensity to form a bubble network is strong at T = 600 K, and decreases systematically with increasing temperature until there is essentially no effect at T = 2000 K.

Acknowledgments

L.S., D.P., and B.P.U. acknowledge support by the U.S. DOE, Office of Science, Office of Fusion Energy Sciences, and Office of Advanced Scientific Computing Research through the Scientific Discovery through Advanced Computing (SciDAC) project on Plasma-Surface Interactions. A.F.V. was supported

by the U.S. DOE, Office of Basic Energy Sciences, Materials Sciences and Engineering Division. This research used resources of the National Energy Research Scientific Computing Center, which is supported by the Office of Science of the U.S. DOE under Contract No. DE-AC02-05CH11231, and resources of the Oak Ridge Leadership Computing Facility at Oak Ridge National Laboratory, which is supported by the Office of Science of the U.S. DOE under Contract No. DE-AC05- 00OR22725. Los Alamos National Laboratory is operated by Los Alamos National Security, LLC, for the National Nuclear Security Administration of the U.S. DOE, under Contract No. DE-AC52-O6NA25396.

References

[1] D. M. Duffy, Modeling plasma facing materials for fusion power, Mater. Today 12 (2009) 38–44.

[2] J. Marian, C. S. Becquart, C. Domain, S. L. Dudarev, M. R. Gilbert, R. J. Kurtz, D. R. Mason, K. Nordlund, A. E. Sand, L. L. Snead, T. Suzudo, B. D. Wirth, Recent advances in modeling and simulation of the exposure and response of tungsten to fusion energy conditions, Nucl. Fusion 57 (2017) 092008.

[3] G. Pintsuk, 4.17 - Tungsten as a Plasma-Facing Material, in: R. Konings (Ed.), Comprehensive Nuclear Materials, Elsevier, 551, 2012.

[4] M. J. Baldwin, R. P. Doerner, Formation of helium induced nanostructure 'fuzz' on various tungsten grades, J. Nucl. Mater. 404 (2010) 165–173.

[5] H. Iwakiri, K. Yasunaga, K. Morishita, N. Yoshida, Microstructure evolution in tungsten during low-energy helium ion irradiation, J. Nucl. Mater. 283-287 (2000) 1134–1138.

[6] G. Valles, I. Martin-Bragado, K. Nordlund, A. Lasa, C. Björkas, E. Safi, J. M. Perlado, A. Rivera, Temperature dependence of underdense nanostructure formation in tungsten under helium irradiation, J. Nucl. Mat. 490 (2017) 108–114.

[7] V. Borovikov, A. F. Voter, X.-Z. Tang, Reflection and implantation of low energy helium with tungsten surfaces, J. Nucl. Mater. 447 (2014) 254–270.

[8] P. E. Lhuillier, T. Belhabib, P. Desgardin, B. Courtois, T. Sauvage, M. F. Barthe, A. L. Thomann, P. Brault, Y. Tessier, Helium retention and early stages of helium-vacancy complexes formation in low energy helium-implanted tungsten, J. Nucl. Mater. 433 (2013) 305–313.

[9] D. Perez, T. Vogel, B. P. Uberuaga, Diffusion and transformation kinetics of small helium clusters in bulk tungsten, Phys. Rev. B 90 (2014) 014102.

[10] W. D. Wilson, C. L. Bisson, M. I. Baskes, Self-trapping of helium in metals, Phys. Rev.B 24 (1981) 5616–5624.

[11] J. Baštecká, Interaction of dislocation loop with free surface, Cechoslovackij fiziceskij zurnal B 14 (1964) 430–442.

[12] P. P. Groves, D. J. Bacon, The dislocation loop near a free surface, Philos. Mag. 22 (1970) 83–91.

[13] S. M. Ohr, Elastic fields of a dislocation loop near a stress-free surface, J. Appl. Phys. 49 (1978) 4953–4955.

[14] D. Perez, L. Sandoval, B. P. Uberuaga, A. F. Voter, The thermodynamic and kinetic interactions of He interstitial clusters with bubbles in W, J. Appl. Phys. 119 (2016) 203301.

[15] E. V. Kornelse, The interaction of injected helium with lattice defects in a tungsten crystal, Radiat. Eff. 13 (1972) 227–236.

[16] N. Juslin, V. Jansson, K. Nordlund, Simulation of cascades in W-He, Philos. Mag. 90 (2010) 3581–3589.

[17] R. Kobayashi, T. Hattori, T. Tamura, S. Ogata, A molecular dynamics study on bubble growth in tungsten under helium irradiation, J. Nucl. Mater. 463 (2015) 1071–1074.

[18] R. D. Smirnov, S. I. Krasheninnikov, J. Guterl, Atomistic modeling of growth and coalescence of helium nano-bubbles in tungsten, J. Nucl. Mater. 463 (2015) 359–362.

[19] S. I. Krasheninnikov, R. D. Smirnov, He cluster dynamics in W in the presence of cluster induced formation of He traps, Physica Scripta T167 (2016) 014021.

[20] B. D. Wirth, Private communication. Our set of simulation parameters comes from unplublished data calculated with Xolotl (https://xolotl-psi.sourceforge.io/), 2017.

[21] J. Roth, E. Tsitrone, A. Loarte, T. Loarer, G. Counsell, R. Neu, V. Philipps, S. Brezinsek, M. Lehnen, P. Coad, C. Grisolia, K. Schmid, K. Krieger, A. Kallenbach, B. Lipschultz, R. Doerner, R. Causey, V. Alimov, W. Shu, O. Ogorodnikova, A. Kirschner, G. Federici, A. Kukushkin, Recent analysis of key plasma wall Interactions issues for ITER, J. Nucl. Mater. 390-391 (2009) 1–9.

[22] S. Plimpton, Fast parallel algorithms for short-range molecular dynamics, J. Comp. Phys. 117 (1995) 1–19.

[23] G. J. Ackland, R. Thetford, An improved N-body semi-empirical model for body-centred cubic transition metals, Phil. Mag. A 56 (1987) 15–30.

[24] N. Juslin, B. D. Wirth, Interatomic potentials for simulation of He bubble formation in W, J. Nucl. Mater. 432 (2013) 61–66.

[25] D. E. Beck, A new interatomic potential function for helium, Mol. Phys. 15 (1968) 311–315.

[26] K. Morishita, R. Sugano, B. D. Wirth, T. Díaz de la Rubia, Thermal stability of helium-vacancy clusters in iron, Nucl. Instrum. Meth. B 202 (2003) 76–81.

[27] A. Stukowski, Visualization and analysis of atomistic simulation data with OVITO–the Open Visualization Tool, Modelling Simul. Mater. Sci. Eng. 18 (2010) 015012.

[28] D. Perez, L. Sandoval, S. Blondel, B. D. Wirth, B. P. Uberuaga, A. F. Voter, The mobility of small vacancy/helium complexes in tungsten and its impact on retention in fusion-relevant conditions, Sci. Rep. 7 (2017) 2522.

[29] L. Sandoval, D. Perez, B. P. Uberuaga, A. F. Voter, Competing kinetics and He bubble morphology in W, Phys. Rev. Lett. 114 (2015) 105502.

[30] M. Miyamoto, S. Mikami, H. Nagashima, N. Iijima, D. Nishijima, R. P. Doerner, N. Yoshida, H. Watanabe, Y. Ueda, A. Sagara, Systematic investigation of the formation behavior of helium bubbles in tungsten, J. Nucl. Mater. 463 (2015) 333–336.

[31] E. Bernard, R. Sakamoto, M. Tokitani, S. Masuzaki, H. Hayashi, H. Yamada, N. Yoshida, Temperature impact on the micro structure of tungsten exposed to He irradiation in LHD, J. Nucl. Mater. 484 (2017) 24–29.

[32] J. Boisse, A. De Backer, C. Domain, C. S. Becquart, Modeling of the self trapping of helium and the trap mutation in tungsten using DFT and empirical potentials based on DFT, J. Mater. Res. 29 (2014) 2374–2386.

a) Only monomers

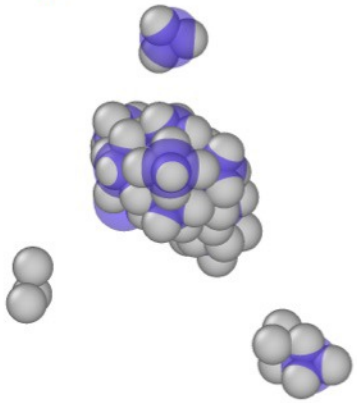

$H_{63}V_{12}$ at 600 K

b) Monomers and dimers

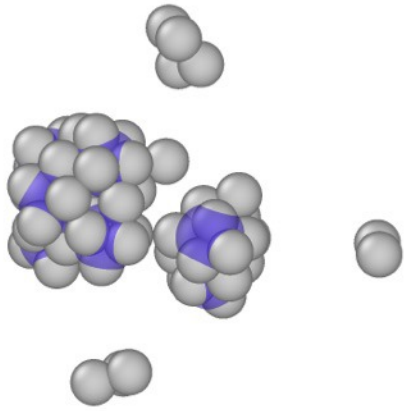

$H_{63}V_{8}$ at 600 K

c)

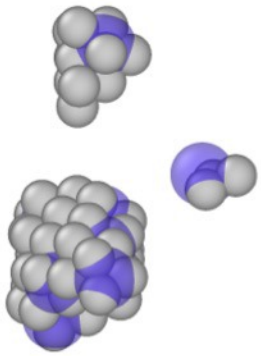

$H_{63}V_{16}$ at 1000 K

d)

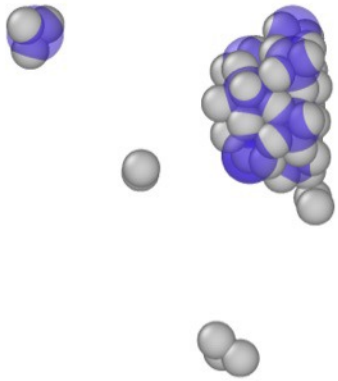

$H_{63}V_{16}$ at 1000 K

e)

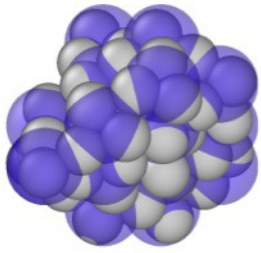

$H_{63}V_{21}$ at 1600 K

f)

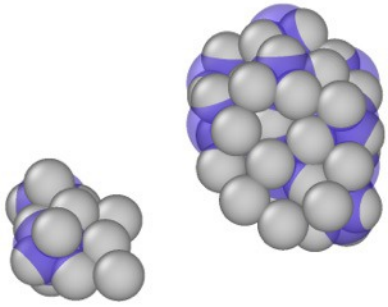

$H_{63}V_{12}$ at 1600 K

g)

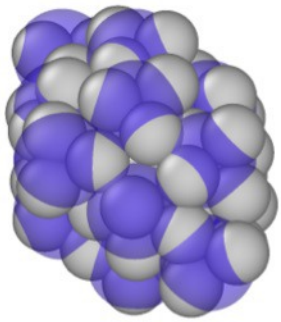

$H_{63}V_{17}$ at 2000 K

h)

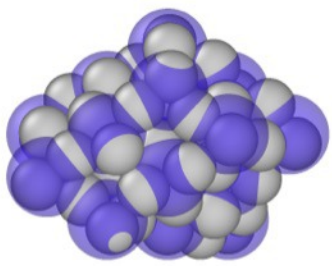

$H_{63}V_{20}$ at 2000 K